Development of an electrochemiluminescent oligonucleotide-based assay for the quantification of prostate cancer associated miR-141-3p in human serum

Development of an electrochemiluminescent oligonucleotide-based assay for the quantification of prostate cancer associated miR-141-3p in human serum

Rui Campos[a,b,1,*], Saranya Thiruvottriyur Shanmugam[a,b], Elise Daems[a,b], Ricardo Ribeiro[c,d] and Karolien De Wael[a,b]

[a] A-Sense Lab, Department of Bioscience Engineering, University of Antwerp, Groenenborgerlaan 171, 2020, Antwerp, Belgium

[b] NANOlab Center of Excellence, University of Antwerp, Groenenborgerlaan 171, 2020, Antwerp, Belgium

[c] i3S, Tumour & Microenvironment Interactions Group, Instituto de Investigação e Inovação em Saúde, University of Porto, Rua Alfredo Allen 208, 4200-135 Porto, Portugal

[d] Department of Pathology, Centro Hospitalar Universitário do Porto, Largo Prof. Abel Salazar, 4099-001 Porto, Portugal

[1] Current address: Food Quality and Safety Group, International Iberian Nanotechnology Laboratory (INL), Av. Mestre José Veiga, 4715-330 Braga, Portugal

[*]Corresponding author: rui.campos@inl.int

Abstract

MicroRNAs (miRNAs) are small oligonucleotides (18-25 bases), biologically relevant for epigenetic regulation of key processes, particularly in association with cancer. Research effort has therefore been directed towards the monitoring and detection of miRNAs to progress (early) cancer diagnoses. Traditional detection strategies for miRNAs are expensive, with a lengthy time-to-result. In this study we develop an oligonucleotide-based assay using electrochemistry for the specific, selective and sensitive detection of a circulating miRNA (miR-141) associated with prostate cancer. In the assay, the excitation and readout of the signal are independent: an electrochemical stimulation followed by an optical readout. A 'sandwich' approach is incorporated, consisting of a biotinylated capture probe immobilised on streptavidin-functionalised surfaces and a detection probe labelled with digoxigenin. We show that the assay allows the detection of miR-141 in human serum, even in the presence of other miRNAs, with a LOD of 0.25 pM. The developed electrochemiluminescent assay has, therefore, the potential for efficient universal oligonucleotide target detection via the redesign of capture and detection probes.

Graphical Abstract

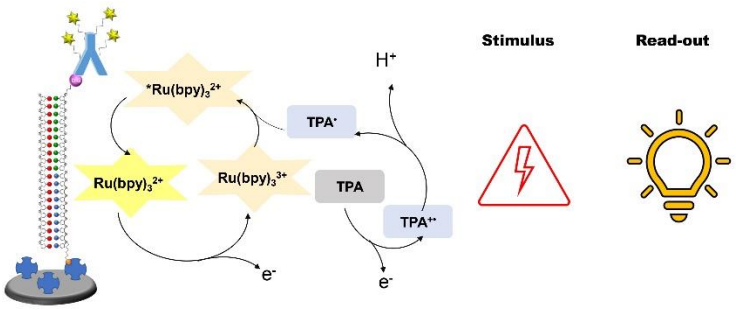

Keywords

Electrochemiluminescence; miRNAs; prostate cancer; liquid biopsy

1. Introduction

Currently, the standard practice for cancer diagnosis is based on a combination of cross-sectional imaging and tissue biopsies. Imaging techniques elucidate the presence, location and size of a tumour, but lack information regarding tumour grading and molecular characterisation [1]. Therefore, the tissue biopsy is subjected to a histopathological analysis to confirm malignancy and determine the cancer type and subtype. Sometimes, this examination is followed by molecular testing to identify which biomarkers are present and guide personalised treatment plans since patients with certain biomarkers are eligible for a specific targeted therapy. A tissue biopsy is, however, highly invasive and does not account for a tumour's heterogeneity [2]. The use of liquid biopsies opens the possibility to collect biofluids in a minimally invasive way and thus track biomarker levels throughout the disease course and during treatment. Monitoring biomarkers in biofluids allows for increased accuracy in treatment decisions and reactionary treatment strategies, leading to personalised medicine [3,4]. This is particularly important when a change from a drug-sensitive to a drug-resistant disease occurs.

Liquid biopsy allows the detection of various cancer biomarkers, such as circulating tumour cells (CTCs) [5], circulating tumour DNA (ctDNA) [6] and non-coding microRNAs (miRNAs) [7]. Particularly, aberrant amounts of circulating miRNAs have been increasingly shown to have a biological impact and are clinically associated with cancer [8,9]. We have chosen to study miR-141-3p (hereafter miR-141), as this is one of the miRNAs that has been associated with various types of cancer such as prostate, colon and lung [10]. In prostate cancer, miR-141 is overexpressed and its levels can be correlated to the total PSA levels [7,11,12]. In fact, data from clinical studies and meta-analysis demonstrated that the altered expression of miR-141 is consistently associated with prostate cancer aggression, distant metastasis, biochemical recurrence, and prognosis [13,14]. The high chemical stability of these nucleic acids in body fluids makes them powerful biomarkers that are present at levels suitable for testing in biofluid samples from patients [15]. To address the drawbacks of current miRNA detection techniques, research into electrochemiluminescence (ECL) detection of nucleic acids has been gaining momentum.

In ECL, which combines electrochemistry and chemiluminescence, when applying a potential, the ECL label, generally called luminophore, undergoes a high-energy electron-transfer reaction in the presence of a co-reactant, which can generate electronically excited states emitting light. Thus, ECL produces light from an electrochemical stimulus, combining high sensitivity, low background, and fast response [16,17]. The use of ECL for miRNA detection has gained interest in recent years with, in particular, ruthenium-based systems in the presence of a co-reactant such as tripropylamine (TPA) being a textbook example [17,18]. However, there are other ways to improve the ECL signal, such as a two-stage isothermal strand-displacement polymerase reaction [19], and the combination of ECL signal quenchers (namely carbon dots) with a duplex specific nuclease [20]. However, such assays are expensive and complex, thereby limiting their applicability in POC testing.

Recent reports on the ECL detection of miRNAs associated with oncological diseases include those performed by the group of Chai and Yuan [21,22] and the group of Zhou [23]. In their first work [21], the group of Chai and Yuan designed dual miRNAs-fuelled DNA nanogears for detection of the miRNA with a single luminophore. In buffer, miR-155 was detected down to fM levels and detection of the miRNA was also possible in cancer cell lysates, although no quantification was performed in this sample matrix. In their second work [22], the authors developed a DNA walking machine to detect miR-21 and miR-155 but the detection was only

performed in buffer. Even though the work developed by this group is very impressive, it lacks the analysis of clinical samples and that is key in the development of an assay to be used as POC testing. Zhou's group developed an ECL biosensing platform to detect miR-21 and the protein mucin 1 and they were able to detect both targets in human serum [23]. The catalytic hairpin assembly process is initiated by the presence of miR-21, whose presence brings CdS:Mn quantum dots to the electrode surface, leading to an ECL response. The detection of mucin 1 is triggered by its aptamer, which allows Au nanoparticles to approach the CdS:Mn quantum dots leading to a decrease in the ECL signal. This is a very complex architecture, which limits its application in a real setting. The three works discussed above highlight the difficulty of working with clinical samples and confirm that, to date, no routine assay is available to detect miRNAs in serum or plasma from oncological patients. The ECL assay developed here is straightforward, not requiring complex strategies or detection mechanisms.

Amgen Research has reported the quantification of oligonucleotides in biological matrices using a commercially available ECL instrument [24,25]. The use of a sandwich assay, together with locked nucleic acids (LNA) allowed oligonucleotide detection between 0.3 pM and 16.7 nM in serum. Despite the high cost of the assays and the need to home-label the reporting antibody, the promising results lead us to develop a DNA-based sandwich assay for the detection of miR-141 as a term of comparison to the PEC approach we have developed in parallel.

The aim of this work is to develop an ECL assay for the detection and quantification of miR-141 in human serum. We have optimised the assay parameters such as concentration of probes, amount of anti-digoxygenin (anti-DIG) antibody used and optimal serum dilution during hybridisation step. The analytical performance with the optimised parameters has been evaluated for the detection of miR-141 in hybridization buffer and diluted serum. The assay possesses the characteristics that POC assays should display, namely robustness, sensitivity and selectivity while being able to quantify miRNAs in complex biological matrices.

2. Materials and Methods

2.1 Materials

Sodium phosphate monobasic, sodium phosphate dibasic, sodium chloride, magnesium chloride, Tween 20, trizma (Tris) base (2-amino-2-hydroxymethyl-1,3-propane-diol), hydrochloric acid, ethylenediaminetetraacetic Acid (EDTA) and human serum were purchased from Sigma-Aldrich (Overijse, Belgium). DNA and miRNA sequences used in this work were purchased from Eurogentec (Liège, Belgium) and are shown in Table 1. Stock solutions of 100 µM were prepared by reconstitution in ultrapure water (UPW).

Table 1: DNA and RNA sequences used to detect miR141 using an ECL assay. TEG = triethylene glycol.

Name	5' modification	Sequence (5' – 3')	3' modification
Target (miR-141-3p (MIMAT0000432))	-	UAA CAC UGU CUG GUA AAG AUG G	-
Capture probe	Biotin-TEG	CCA TCT TTA CC	-
Detection probe	-	AGA CAG TGT TA	Digoxigenin
Negative Control (miR-375-3p)	-	UUU GUU CGU UCG GCU CGC GUG A	-
Negative Control (miR-145-5p)	-	GUC CAG UUU UCC CAG GAA UCC CU	-

2.2 ECL Assay and preparation

Goat polyclonal anti-DIG antibody (Abcam, Cat. Ab76907) was conjugated with multiple tris(2,2'-bipyridyl) ruthenium(II) ($Ru(bpy)_3^{2+}$) labels using the MSD Gold Sulfo-Tag NHS-Ester conjugation kit (Meso Scale Diagnostics, R31AA-1, protocol in section 1.1 in Supplementary Information). MSD GOLD 96-well Streptavidin QUICKPLEX Plate Pack (L55SA), MSD GOLD 96-well Small Spot Streptavidin SECTOR Plate (L45SA) and MSD GOLD Read Buffer (R92TG) were purchased from Meso Scale Discovery, USA.

Before the immobilisation on the well plate, the three strands forming the sandwich were allowed to react for one hour at room temperature in hybridisation buffer (5 mM Tris, 0.5 mM EDTA, 1 M NaCl and 0.05% Tween20, pH 7.5 adjusted using HCl) or diluted serum (1:2, 1:5, 1:10, 1:20 or 1:50 serum:hybridisation buffer) (Figure 1A). Unless stated otherwise, the concentrations of capture and detection probe were 24 nM and the concentration of the target varied from 24 nM to 1.5 pM (8 dilutions with a 5-fold ratio, including a non-target control). Upon reaction, 50 µL of the master mix was transferred to a well, that had previously been washed once with 150 µL of PBS-T (1.8 mM KH_2PO_4 + 10 mM Na_2HPO_4 + 2.7 mM KCl and 137 mM NaCl with 0.05% Tween 20) and tap-dried, allowing to interact for one hour at room temperature at 550 rpm in a plate shaker. The plate was then washed three times with 150 µL PBS-T and tap-dried before adding 25 µL of anti-DIG antibody solution. After one hour of reaction, the plate was washed again three times with 150 µL PBS-T and tap-dried. Then 150 µL of MSD GOLD Read Buffer A, containing the co-reactant TPA, was added and the plate was read immediately in the MSD Quick Plex SQ 120 controlled by the Methodical Mind reader software (Figure 1B).

To assess the specificity and the selectivity of the probes, ECL measurements were performed in the presence of negative controls (another miRNA), instead of the desired target, and in a mixture containing the target and two other RNA strands, respectively. The standard curves, in both hybridisation buffer and serum, obtained in these conditions, were compared to those obtained in the presence of the target only.

3. Results and Discussion

In this work we have evaluated the ECL response of the duplex formed by the target miRNA (miR-141) hybridised with the capture and detection probe in a sandwich-like format (Figure 1A). The streptavidin-modified electrodes trap the sandwich duplex via the biotinylated capture probe. The detection probe is labelled with DIG and will be recognised by the $Ru(bpy)_3^{2+}$-labelled anti-DIG antibody which is in close proximity to the electrode surface for the ECL reaction in presence of the co-reactant TPA (Figure 1B). The oxidation of TPA generates the TPA radical cation ($TPA^{\bullet+}$) that undergoes deprotonation, resulting in the formation of the TPA radical ($TPA^{\bullet}$). $TPA^{\bullet}$ is a strong reducing species that reacts with the electrogenerated $Ru(bpy)_3^{3+}$ to form the $Ru(bpy)_3^{2+}$ excited state which emits light [25–28]. The emission depends on the $Ru(bpy)_3^{2+}$ concentration which is directly proportional to the concentration of the anti-DIG antibody, and in-turn the target miRNA.

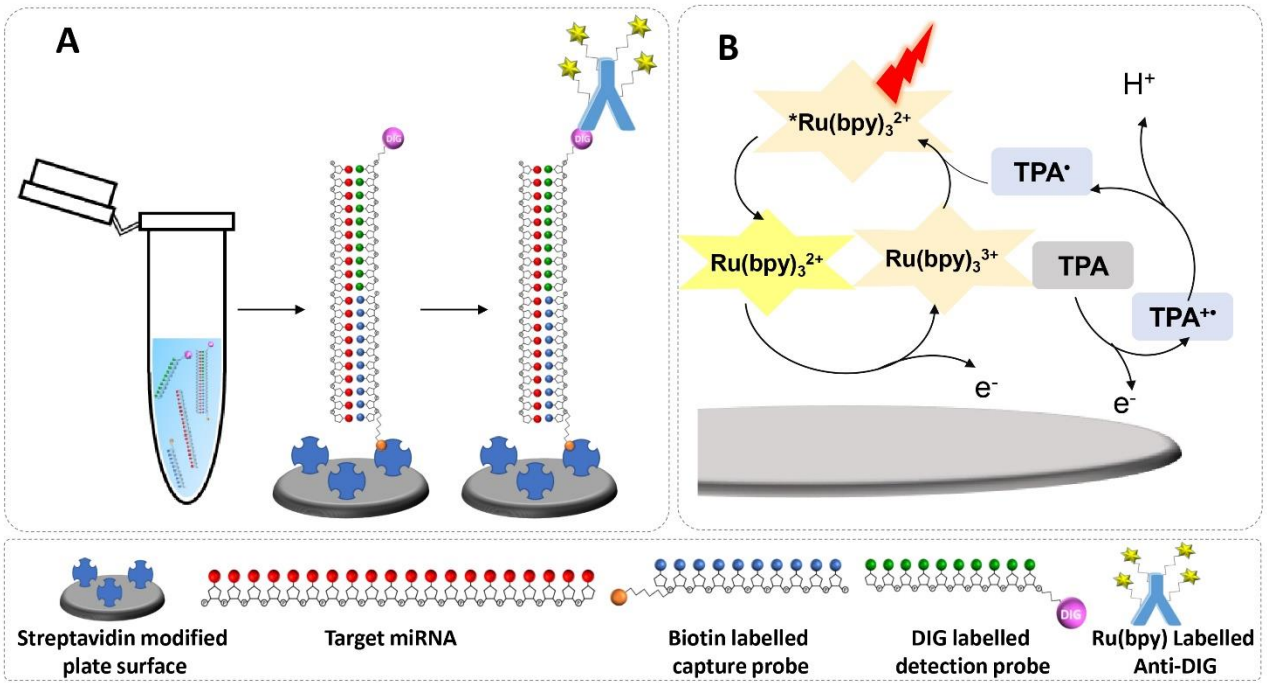

Figure 1 – Schematic representation of A) the developed ECL oligonucleotide based assay and B) its detection mechanism. The lower panel shows the various components of the assay.

3.1 ECL Assay

3.1.1 Optimisation of parameters

With an aim to develop an oligonucleotide-based ECL assay to detect miR-141, we initially optimised the concentration of capture and detection probes, the amount of anti-DIG antibody and the serum dilution. The ECL plate supplier indicates that the binding capability of the plate is 0.3 pmol/well, measured by titrating the plate with biotin-tagged immunoglobuline G (IgG), which corresponds to a concentration of biotinylated capture probe of 6 nM (the volume used in the well was 50 µL). Because the binding capability was determined for IgG, and not for oligonucleotides, higher concentrations of oligo (12 nM and 24 nM) were also tested. As can be seen in Figure 2A, 24 nM allowed the detection of target at higher concentrations without saturation of the signal, so we decided to perform all the following experiments with this concentration of capture and detection probes. Next, the concentration of anti-DIG antibody was varied between 0.5 and 2 µg/mL (Figure 2B). The concentration of antibody has no significant effect on the ECL counts. Consequently, the lowest concentration of anti-DIG antibody (0.5 µg/mL) was used during the remainder of the experiments.

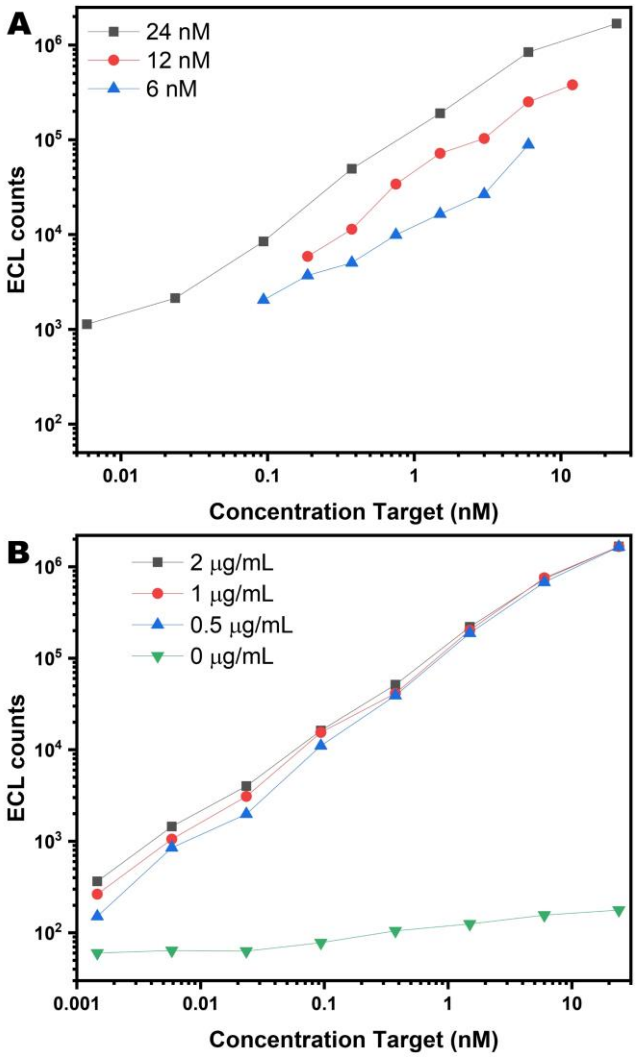

Figure 2 – Optimisation of various parameters to be used in the ECL assay for the detection of miR-141. A) Concentration of probe and B) amount of anti-DIG antibody. Mean data is shown with error bars representing standard deviation (n=2). Axes are in log scale.

To investigate the influence of the serum matrix on the hybridisation of the sandwich assay, the hybridisation with different concentrations of target (miR-141) was performed in various dilutions of serum (1:2, 1:5, 1:10, 1:20 and 1:50, serum: hybridisation buffer ratio). As can be seen in Figure 3, only at a 1:20 and 1:50 ratio it is possible to detect the target miRNA at the pM level. For the other dilutions with high concentrations of serum, matrix effects from high concentrations of serum prevented the generation of ECL signal. Though the measurements are performed in measuring buffer, during the hybridisation step, most likely, proteins in the serum at higher concentrations foul the electrode surface and remain on the surface even after the washing steps, thus passivating the surface. We opted for the dilution 1:20 since it gives similar results to the dilution 1:50 and means a lower dilution of the target. The same dilution has been used by Thayer *et al.* for the detection of siRNA in human excreta when using an instrument from Meso Scale Discovery [24,25].

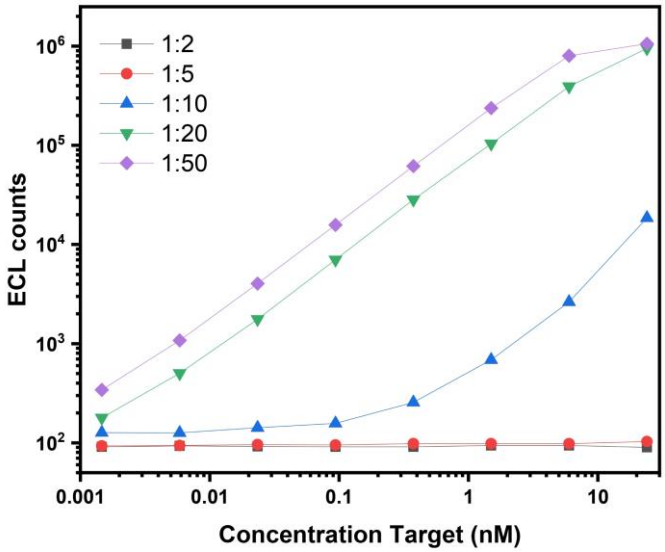

Figure 3 – Optimisation of the serum dilution to be used in the ECL assay for the detection of miR-141. The serum was diluted with hybridization buffer in a 1:2, 1:5, 1:10, 1:20, and 1:50 serum:buffer ratio. Mean data is shown with error bars representing standard deviation (n=2). Axes are in log scale.

3.1.2 Analytical performance in buffer and diluted serum

After optimisation of the parameters, we evaluated the analytical performance of our ECL sandwich assay in hybridisation buffer and in diluted serum (1:20 dilution) during the hybridisation step (Figure 4). Apart from varying the concentration of the targets and building a (i) calibration plot, we tested two controls such as (ii) negative control, by varying the concentration of the target not complementary to the capture and detection probes, and (iii) specificity, by measuring the different concentrations of target in the mixture with 24 nM of two other miRNAs. For this purpose, three different target solutions were tested: (i) miR-141, (ii) miR-145-5p as a negative control, and (iii) miR-141 in the presence of 24 nM of two other miRNAs (miR-145-5p and miR-375-3p). The concentration of miR-141 ranged from 1.5 pM to 24 nM in both buffer and diluted serum. In the first control (called negative control), the concentration of miR-145-5p, which is not complementary to the capture and detection probes, was varied between 1.5 and 24 nM. Addition of this target did not result in an ECL response for buffer and diluted serum, clearly indicating that the probes are specific for miR-141. The second control test (termed specificity) shows that different concentrations of miR-141 can be detected in a mixture with two other miRNAs (miR-145-5p and miR-375-3p), with the detection range not being affected. The ECL assay demonstrates good specificity with an ECL response proportional to the concentration of miR-141 and negligible ECL counts for the negative control. These observations are valid for the assays performed in buffer and in diluted serum, where it is shown linearity within the tested range with good differentiation in signal between the tested concentrations.

Another interesting remark is that the matrix did not have an effect on the detection range of the assay, with the target being detected between 1.5 pM and 24 nM in both buffer and diluted serum. The detectability (lowest detected concentration 1.5 pM) decreased by only 1.6 times in serum in agreement with the complexity of the matrix. The limit of detection (LOD) in buffer was calculated to be 0.12 pM and calculated from the slope (157787 ECL counts/nM, LOD =3*S.D_{blank}/slope) of the calibration curve in the range 0.005 nM –1.5 nM. While in diluted serum, a LOD of 0.25 pM was calculated from the slope (84412 ECL counts/nM, LOD =3*S.D_{blank}/slope) of the calibration curve in the range 0.005 nM – 1.5 nM. Most of the works in literature report levels of miRNAs as relative quantities (e.g.: [29,30]), nevertheless it has been reported that healthy individuals present concentrations of miR-141-3p in the high fM range while prostate cancer patients can

present concentrations up to the low nM [31]. Hence the ECL assay developed in this work is indeed suitable for the detection of miRNAs .

Thus, we successfully demonstrated the analytical performance of our ECL assay with advantages from the specificity of a sandwich assay and the sensitivity of ECL detection. The use of a 96-well plate for the detection allows high throughput and could easily be transferred to a POC setting.

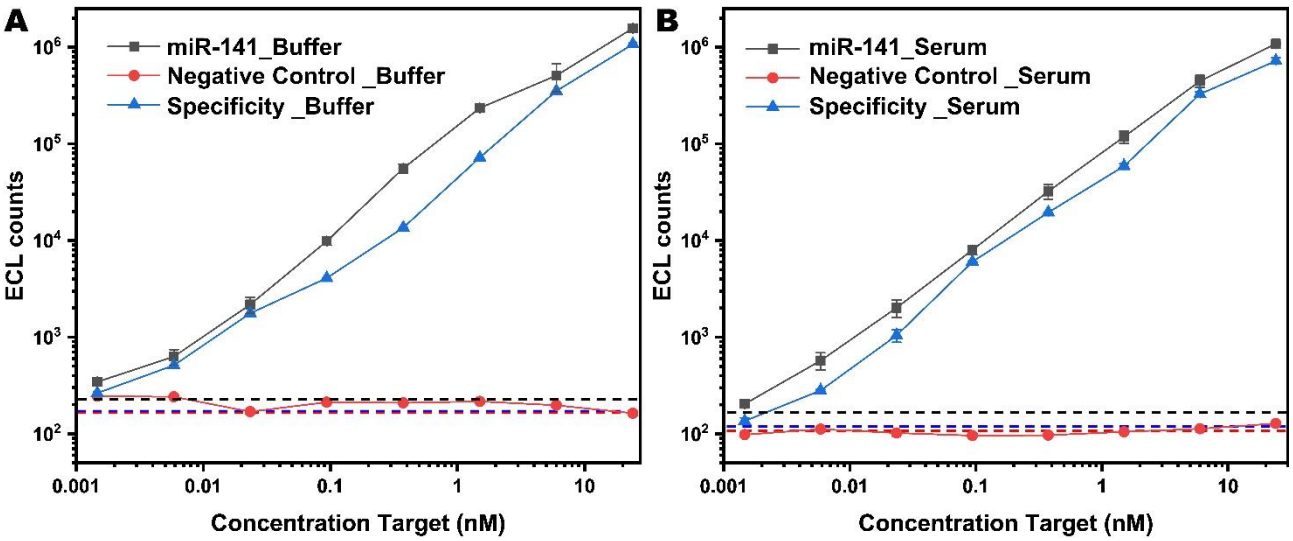

Figure 4 – ECL detection of miR-141 with the hybridization performed in (A) hybridization buffer and in (B) 1:20 human serum. Mean data is shown with error bars representing standard deviation (n=2). Axes are in log scale. The dashed lines correspond to the zero concentration of target of the respective condition. The negative control was performed by varying the concentration of a target not complementary to the capture and detection probes and the specificity assessment was done by measuring different concentrations of target in a mixture containing 24 nM both miR-145-5p and miR-375-3p.

4. Conclusions

In this work, we successfully developed an oligonucleotide based ECL assay for the detection of miRNAs in human serum. The ECL assay showed the ability to detect the target miR-141 at pM levels in human serum. The assay owes its robustness to simple design, specificity of the sandwich format and sensitivity to signal amplification provided by the $Ru(bpy)_3^{3+}$-TPA system. Combining these characteristics allowed the detection of miR-141 in human serum at clinically relevant levels.

The accomplishments of this work pave the way for the construction of a multiple analyte platform that could allow faster and simpler detection of many cancer-related miRNAs. The developed assay has the potential for universal oligonucleotide detection by redesigning the capture and detection probes. It can also be applied to other matrices and, optimally, avoids pre-treatment of the sample.

Declaration of Competing Interest

The authors declare that they have no known competing financial interests or personal relationships that could have appeared to influence the work reported in this article.

Acknowledgements

This work was supported by an individual fellowship of the Marie Skłodowska-Curie Actions to RC (grant number: 842219) and BOF-DOCPRO to STS. We acknowledge FWO for funding. The authors wish to

acknowledge Dr Deborah Decrop, from MSD, for her help with the MSD quickplex instrument and MSD for lending us the equipment. We would also like to acknowledge Dr Peter Tougaard and Prof. Dr Peter Vandenabeele for allowing us to use the MSD quickplex instrument at VIB-UGENT, PT also assisted in some measurements.

References

[1] J. Desroches, M. Jermyn, M. Pinto, F. Picot, M.A. Tremblay, S. Obaid, E. Marple, K. Urmey, D. Trudel, G. Soulez, M.C. Guiot, B.C. Wilson, K. Petrecca, F. Leblond, A new method using Raman spectroscopy for in vivo targeted brain cancer tissue biopsy, Sci. Rep. 8 (2018) 1792. https://doi.org/10.1038/s41598-018-20233-3.

[2] A.P. Sokolenko, E.N. Imyanitov, Molecular Diagnostics in Clinical Oncology, Front. Mol. Biosci. 5 (2018) 76. https://www.frontiersin.org/articles/10.3389/fmolb.2018.00076.

[3] H. Schwarzenbach, D.S.B. Hoon, K. Pantel, Cell-free nucleic acids as biomarkers in cancer patients, Nat. Rev. Cancer. 11 (2011) 426–437. https://doi.org/10.1038/nrc3066.

[4] J.J. Nieva, P. Kuhn, Fluid biopsy for solid tumors: A patients companion for lifelong characterization of their disease, Futur. Oncol. 8 (2012) 989–998. https://doi.org/10.2217/fon.12.91.

[5] V. Akpe, T.H. Kim, C.L. Brown, I.E. Cock, Circulating tumour cells: a broad perspective, J. R. Soc. Interface. 17 (2020) 20200065. https://doi.org/10.1098/rsif.2020.0065.

[6] M.C. Maia, M. Salgia, S.K. Pal, Harnessing cell-free DNA: plasma circulating tumour DNA for liquid biopsy in genitourinary cancers, Nat. Rev. Urol. 17 (2020) 271–291. https://doi.org/10.1038/s41585-020-0297-9.

[7] M.A. Jafri, M.H. Al-Qahtani, J.W. Shay, Role of miRNAs in human cancer metastasis: Implications for therapeutic intervention, Semin. Cancer Biol. 44 (2017) 117–131. https://doi.org/10.1016/J.SEMCANCER.2017.02.004.

[8] L. Fabris, Y. Ceder, A.M. Chinnaiyan, G.W. Jenster, K.D. Sorensen, S. Tomlins, T. Visakorpi, G.A. Calin, The Potential of MicroRNAs as Prostate Cancer Biomarkers, Eur. Urol. 70 (2016) 312–322. https://doi.org/10.1016/j.eururo.2015.12.054.

[9] D. Vanacore, M. Boccellino, S. Rossetti, C. Cavaliere, C. D'Aniello, R. Di Franco, F.J. Romano, M. Montanari, E. La Mantia, R. Piscitelli, F. Nocerino, F. Cappuccio, G. Grimaldi, A. Izzo, L. Castaldo, M.F. Pepe, M.G. Malzone, G. Iovane, G. Ametrano, P. Stiuso, L. Quagliuolo, D. Barberio, S. Perdonà, P. Muto, M. Montella, P. Maiolino, B.M. Veneziani, G. Botti, M. Caraglia, G. Facchini, Micrornas in prostate cancer: An overview, Oncotarget. 8 (2017) 50240–50251. https://doi.org/10.18632/oncotarget.16933.

[10] E. Endzeliņš, V. Melne, Z. Kalniņa, V. Lietuvietis, U. Riekstiņa, A. Llorente, A. Line, Diagnostic, prognostic and predictive value of cell-free miRNAs in prostate cancer: A systematic review, Mol. Cancer. 15 (2016) 1–13. https://doi.org/10.1186/s12943-016-0523-5.

[11] W. Jin, X. Fei, X. Wang, F. Chen, Y. Song, Circulating miRNAs as Biomarkers for Prostate Cancer Diagnosis in Subjects with Benign Prostatic Hyperplasia, J. Immunol. Res. 2020 (2020) ID 5873056. https://doi.org/10.1155/2020/5873056.

[12] A.H. Zedan, P.J.S. Osther, J. Assenholt, J.S. Madsen, T.F. Hansen, Circulating miR-141 and miR-375 are associated with treatment outcome in metastatic castration resistant prostate cancer, Sci. Reports 2020 101. 10 (2020) 1–9. https://doi.org/10.1038/s41598-019-57101-7.

[13] J.C. Gonzales, L.M. Fink, O.B. Goodman, J.T. Symanowski, N.J. Vogelzang, D.C. Ward, Comparison of circulating MicroRNA 141 to circulating tumor cells, lactate dehydrogenase, and prostate-specific antigen for determining treatment response in patients with metastatic prostate cancer, Clin. Genitourin. Cancer. 9 (2011) 39–45. https://doi.org/10.1016/j.clgc.2011.05.008.

[14] D. Ye, Z. Shen, S. Zhou, Function of microRNA-145 and mechanisms underlying its role in malignant tumor diagnosis and treatment, Cancer Manag. Res. 11 (2019) 969–979. https://doi.org/10.2147/CMAR.S191696.

[15] T. Blondal, S. Jensby Nielsen, A. Baker, D. Andreasen, P. Mouritzen, M. Wrang Teilum, I.K. Dahlsveen, Assessing sample and miRNA profile quality in serum and plasma or other biofluids, Methods. 59 (2013) S1–S6. https://doi.org/10.1016/j.ymeth.2012.09.015.

[16] R.J. Forster, P. Bertoncello, T.E. Keyes, Electrogenerated Chemiluminescence, Annu. Rev. Anal. Chem. 2 (2009) 359–385. https://doi.org/10.1146/annurev-anchem-060908-155305.

[17] W. Miao, Electrogenerated Chemiluminescence and Its Biorelated Applications, Chem. Rev. 108 (2008) 2506–2553. https://doi.org/10.1021/cr068083a.

[18] J.B. Noffsinger, N.D. Danielson, Generation of Chemiluminescence upon Reaction of Aliphatic Amines with Tris(2,2‘-bipyridine)ruthenium(III), Anal. Chem. 59 (1987) 865–868. https://doi.org/10.1021/ac00133a017.

[19] M. Wang, Y. Zhou, H. Yin, W. Jiang, H. Wang, S. Ai, Signal-on electrochemiluminescence biosensor for microRNA-319a detection based on two-stage isothermal strand-displacement polymerase reaction, Biosens. Bioelectron. 107 (2018) 34–39. https://doi.org/10.1016/j.bios.2018.02.015.

[20] J. Yang, Q. Xia, L. Guo, F. Luo, Y. Dong, B. Qiu, Z. Lin, A highly sensitive signal-on biosensor for microRNA 142-3p based on the quenching of Ru(bpy)32+-TPA electrochemiluminescence by carbon dots and duplex specific nuclease-assisted target recycling amplification, Chem. Commun. 56 (2020) 6692–6695. https://doi.org/10.1039/c9cc09706f.

[21] P. Zhang, Z. Lin, Y. Zhuo, R. Yuan, Y. Chai, Dual micrornas-fueled DNA nanogears: A case of regenerated strategy for multiple electrochemiluminescence detection of micrornas with single luminophore, Anal. Chem. 89 (2017) 1338–1345. https://doi.org/10.1021/acs.analchem.6b04402.

[22] L. Peng, P. Zhang, Y. Chai, R. Yuan, Bi-directional DNA Walking Machine and Its Application in an Enzyme-Free Electrochemiluminescence Biosensor for Sensitive Detection of MicroRNAs, Anal. Chem. 89 (2017) 5036–5042. https://doi.org/10.1021/acs.analchem.7b00418.

[23] J. Li, J. Liu, Y. Bi, M. Sun, J. Bai, M. Zhou, Ultrasensitive electrochemiluminescence biosensing platform for miRNA-21 and MUC1 detection based on dual catalytic hairpin assembly, Anal. Chim. Acta. 1105 (2020) 87–94. https://doi.org/10.1016/j.aca.2020.01.034.

[24] M.B. Thayer, J.M. Lade, D. Doherty, F. Xie, B. Basiri, O.S. Barnaby, N.S. Bala, B.M. Rock, Application of Locked Nucleic Acid Oligonucleotides for siRNA Preclinical Bioanalytics, Sci. Rep. 9 (2019) 1–9. https://doi.org/10.1038/s41598-019-40187-4.

[25] M.B. Thayer, S.C. Humphreys, K.S. Chung, J.M. Lade, K.D. Cook, B.M. Rock, POE Immunoassay: Plate-based oligonucleotide electro-chemiluminescent immunoassay for the quantification of nucleic acids in biological matrices, Sci. Rep. 10 (2020) 10425. https://doi.org/10.1038/s41598-020-66829-6.

[26] W. Miao, J.-P. Choi, A.J. Bard, Electrogenerated Chemiluminescence 69: The Tris(2,2‘-bipyridine)ruthenium(II), (Ru(bpy)32+)/Tri-n-propylamine (TPrA) System RevisitedA New Route Involving TPrA•+ Cation Radicals, J. Am. Chem. Soc. 124 (2002) 14478–14485. https://doi.org/10.1021/ja027532v.

[27] J.K. Leland, M.J. Powell, Electrogenerated Chemiluminescence: An Oxidative-Reduction Type ECL Reaction Sequence Using Tripropyl Amine, J. Electrochem. Soc. 137 (1990) 3127–3131. https://doi.org/10.1149/1.2086171.

[28] K. Hiramoto, E. Villani, T. Iwama, K. Komatsu, S. Inagi, K.Y. Inoue, Y. Nashimoto, K. Ino, H. Shiku, Recent Advances in Electrochemiluminescence-Based Systems for Mammalian Cell Analysis, Micromachines. 11 (2020) 530. https://doi.org/10.3390/mi11050530.

[29] H.C.N. Nguyen, W. Xie, M. Yang, C.-L. Hsieh, S. Drouin, G.-S.M. Lee, P.W. Kantoff, Expression differences of circulating microRNAs in metastatic castration resistant prostate cancer and low-risk, localized prostate cancer, The Prostate 73 (2013) 346-354. https://doi.org/10.1002/pros.22572.

[30] S. Arisan, P. Ozfiliz-Kilbas, O. Rencuzogullari, N.P. Unsal, A. Coker-Gurkan, P. Obakan-Yerlikaya, P. Uysal-Onganer, E.D. Arisan, Circulating microRNA expression profiles to identify a potential link between prostate cancer and obesity, Human Gene 34 (2022) 201109. https://doi.org/10.1016/j.humgen.2022.201109.

[31] A.F.-J. Jou, C.-H. Lu, Y.-C. Ou, S.-S. Wang, S.-L. Hsu, I. Willner, J.-a.A. Ho, Diagnosing the miR-141 prostate cancer biomarker using nucleic acid-functionalized CdSe/ZnS QDs and telomerase, Chem. Sci. 6 (2015) 659-665. https://doi.org/10.1039/C4SC02104E.

Development of an electrochemiluminescent oligonucleotide-based assay for the quantification of prostate cancer associated miR-141-3p in human serum

Rui Campos[a,b,1,*], Saranya Thiruvottriyur Shanmugam[a,b], Elise Daems[a,b], Ricardo Ribeiro[c,d] and Karolien De Wael[a,b]

[a] A-Sense Lab, Department of Bioscience Engineering, University of Antwerp, Groenenborgerlaan 171, 2020, Antwerp, Belgium

[b] NANOlab Center of Excellence, University of Antwerp, Groenenborgerlaan 171, 2020, Antwerp, Belgium

[c] i3S, Tumour & Microenvironment Interactions Group, Instituto de Investigação e Inovação em Saúde, University of Porto, Rua Alfredo Allen 208, 4200-135 Porto, Portugal

[d] Department of Pathology, Centro Hospitalar Universitário do Porto, Largo Prof. Abel Salazar, 4099-001 Porto, Portugal

[1] Current address: Food Quality and Safety Group, International Iberian Nanotechnology Laboratory (INL), Av. Mestre José Veiga, 4715-330 Braga, Portugal

[*]Corresponding author: rui.campos@inl.int

Supplementary information

1. Materials and Methods

1.1. Anti-DIG labelling

A full protocol and more details about the conjugation can be found in the MSD website following:

https://www.mesoscale.com/~/media/files/technical%20notes/msd%20sulfo-tag%20nhs-ester.pdf

SULFO-tag labelling of anti-Digoxigenin antibody (challenge ratio of 20:1)

Pre-Conjugation Procedure

1. Prepare a 1 mg/mL solution of the protein to be conjugated in Conjugation Buffer.

a. Preservatives such as sodium azide or EDTA, buffer components containing primary amines (e.g., Tris, glycine), and glycerol must be removed by buffer exchange using Zeba Spin Desalting Columns that have been equilibrated with Conjugation Buffer before starting the conjugation reaction.

b. Filter the protein using a 0.2 µm filter.

c. Measure the concentration of the protein solution to be conjugated (can be calculated from an OD_{280} absorbance).

2. Equilibrate the protein to be conjugated at the conjugation temperature of 23°C.

3. Calculate the amount of SULFO-TAG NHS-Ester stock solution required.

$$1000 \times \frac{Protein\ Conc.\left(\frac{mg}{mL}\right)}{Protein\ MW\ (Da)} \times Challenge\ ratio \times Vol.of\ protein\ solution = nmol\ of\ SULFO-TAG\ reagent\ required$$

Using this value, one can calculate the volume of MSD GOLD SULFO-TAG stock solution required for the reaction.

$$\frac{nmol\ of\ SULFO-TAG\ reagent\ required}{Conc.of\ SULFO-TAG\ stock\ solution\left(\frac{nmol}{\mu L}\right)} = \mu L\ of\ SULFO-TAG\ stock\ solution\ required\ for\ conjugation\ reaction$$

Table 1 – Calculation of the volume of SULFO-TAG stock solution required and parameters that led to that value.

Protein Conc. (mg/mL)	1
Ab MW (Da)	150000
Challenge ratio	20
Volume of Ab solution (µL)	100
nmol of SULFO-TAG required	**13.33**
Conc. SULFO-TAG stock solution (nmol/µL)	3
µL of SULFO-TAG stock solution required	**4.44**

Conjugation Procedure

1. Immediately prior to use, reconstitute the vial containing 150 nmol SULFO-TAG NHS-Ester with 50 µL of cold distilled water to generate a stock solution of 3 nmol/µL (gently vortex). Reconstituted SULFO-TAG NHS-Ester may be kept for up to 10 min. on ice prior to use.

2. Add the calculated volume of reconstituted SULFO-TAG NHS-Ester to the protein solution and vortex immediately. Discard any remaining SULFO-TAG NHS-Ester.

3. Incubate at 23°C for 2 hours (20–25°C is acceptable). Shield the reaction from light by covering the tube with aluminium foil or placing it in a dark area (e.g., a closed drawer).

Post-Conjugation Procedure

1. Prepare Zeba Spin Desalting Columns. Remove the storage buffer and wash the column 3 times with MSD Conjugate Storage Buffer. 2. Apply the conjugation reaction to the centre of the spin column. Centrifuge the column in clean, new collection tube to purify the SULFO-TAG conjugated protein. The SULFO-TAG conjugated protein will be present in the eluate in the collection tube (discard the columns).

3. Filter the conjugated protein using a 0.2 µm filter.

4. The molar protein concentration of the conjugated protein was determined using a Bradford colorimetric protein assay. (= 0.32 mg/mL)

5. The absorbance of the MSD SULFO-TAG protein conjugate was measured at 455 nm using a nanodrop spectrophotometer. (OD = 0.6, optical path length = 1.005 cm)

6. Follow the calculations below to determine the SULFO-TAG label:protein conjugation ratio.

$$\frac{Protein\ conc.\left(\frac{mg}{mL}\right)}{Protyein\ MW\ (Da)} = \cdots M\ (A)$$

$$\frac{OD_{455}}{15400\ (extinction\ coefficient) \times optical\ path\ length(cm)} = \cdots M\ (B)$$

A = 2.13×10^{-6} M B = 3.88×10^{-5} M

Labeling incorporation ratio (SULFO-tag label:Protein) = (B/A) = 18.2

MSD SULFO-TAG conjugated proteins may be sensitive to extended exposure to light and should be stored in the dark or in amber or opaque vials. Antibody conjugates are usually stable for at least 2 years at 2–8°C in conjugate storage buffer.